

Conservation-Based Modeling and Boundary Control of Congestion with an Application to Traffic Management in Center City Philadelphia

Xun Liu and Hossein Rastgoftar

Abstract—This paper develops a conservation-based approach to model traffic dynamics and alleviate traffic congestion in a network of interconnected roads (NOIR). We generate an NOIR by using the Simulation of Urban Mobility (SUMO) software based on the real street map of Philadelphia Center City. The NOIR is then represented by a directed graph with nodes identifying distinct streets in the Center City area. By classifying the streets as inlets, outlets, and interior nodes, the model predictive control (MPC) method is applied to alleviate the network traffic congestion by optimizing the traffic inflow and outflow across the boundary of the NOIR. The proposed boundary control problem is defined as a quadratic programming problem with constraints imposing the feasibility of traffic coordination, and a cost function defined based on the traffic density across the NOIR.

I. INTRODUCTION

In the process of urbanization and the rapid popularization of private vehicles, the problem of urban traffic congestion has become more and more prominent and produced numerous negative impacts on economy [1], [2] and environment [3], [4]. Traffic congestion can destroy the urban environment and ecology. Due to the low-speed driving conditions, the emission of greenhouse gas, noxious gas and noise will increase, and that will badly affect human health [5].

Over the past decades, a large number of scholars have developed prediction, control, and optimization methods to solve the challenges of traffic congestion in urban areas. Ref. [6] offers an integration of fuzzy rule-based systems and the genetic algorithms to model and predict the traffic coordination. Refs. [7] and [8] develop the traffic predictive approaches by relying on driver behavior and bus driving intervals. With the rapid development of V2X and autonomous driving technology, floating car data (FCD) technology has been widely used to estimate the traffic state [9], [10].

Researchers have also developed different model-based and model-free approaches to obtain dynamics of traffic coordination and control congestion.

The model-based macroscopic fundamental diagram (MFD), whose applicability for urban traffic is experimentally verified in [11], is an efficient tool to obtain dynamics of an urban traffic network. Ref. [12] applies the MFD model to evaluate the traffic accumulation amount, and estimate the traffic state. Refs. [13], [14] integrate MFD with perimeter control to improve the mobility of a traffic network. Moreover, Refs. [15]–[19] integrate the cell transmission model (CTM) method, which is applied to divide the traffic network

The authors are with the Department of Mechanical Engineering at Villanova University, Villanova, PA 19085, USA {xliu8, hossein.rastgoftar}@villanova.edu

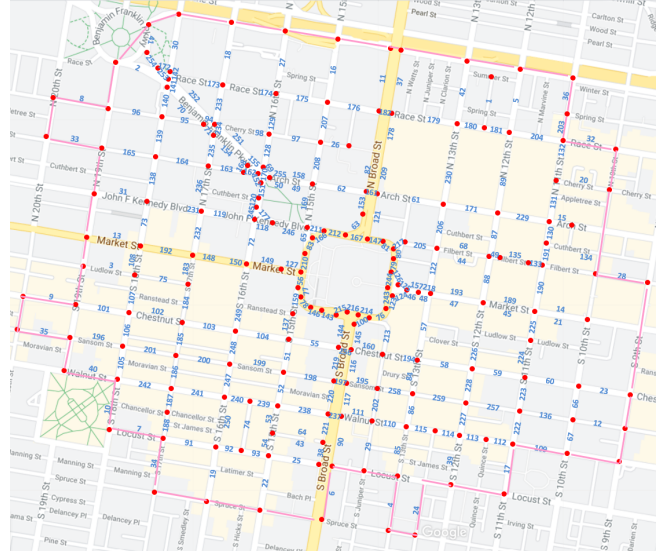


Fig. 1: Example NOIR: Center City, Philadelphia

into homogeneous road elements, with the MFD approach to enhance the efficiency and accuracy of the network modeling. With the improvement of computing capacity and the development of AI technology, reinforcement learning (RL) method has attracted more and more attention. Ref. [20] presents an overview of the recently-developed RL algorithms in the area of adaptive traffic signal control. In Refs. [21]–[24], researchers integrate the model-free methods with RL approaches to optimally plan the functionalities of traffic signals. The model predictive control (MPC) is another commonly used tool for controlling the traffic dynamics in urban networks. Refs. [14], [13], [25], [26] and [27] apply the MPC approach to assign optimal boundary control variables. Ref. [28] integrates the MPC and mixed-integer linear programming (MILP) to manage the complexity of traffic coordination optimization.

This paper offers an integration of mass conservation law and MPC-based boundary control to obtain the traffic dynamics and alleviate the traffic congestion. We use the Simulation of Urban Mobility (SUMO) software to convert the real street map data into a directed graph representing a network of inter-connected roads (NOIR). By classifying the nodes of the generated graph as inlets, outlets, and interior nodes, we apply the mass conservation law to model the traffic coordination as a non-stationary stochastic process, and obtain the traffic feasibility conditions at the interior nodes. Additionally, we apply the MPC to control the boundary

inflow, through the NOIR inlets, and the boundary outflow, through the NOIR outlets. For the case study, we use the proposed model and control approach to evaluate congestion management in a certain area of Center City Philadelphia with the map shown in Fig. 1.

This paper is arranged in the following structure: Section II explains the preliminary notions of graph theory. The problem statement is presented in Section III and followed by obtaining the traffic network dynamics and providing the feasibility conditions in Section IV. Section V presents the boundary control approach based on the MPC method to control the traffic congestion. Then, the simulation results are reported in Section VI and followed by the conclusion in Section VII.

II. PRELIMINARY NOTIONS OF GRAPH THEORY

An NOIR is represented by graph $\mathcal{G}(\mathcal{V}, \mathcal{E})$ where \mathcal{V} and $\mathcal{E} \subset \mathcal{V} \times \mathcal{V}$ define nodes and edges of graph \mathcal{G} , respectively. Node $i \in \mathcal{V}$ represents an NOIR road element where each road element is a one-way street connecting two consecutive junctions (See Fig. 1). Edge $(i, j) \in \mathcal{E}$ represents a directed connection from road element $i \in \mathcal{V}$ to road element $j \in \mathcal{V}$.

Set \mathcal{V} can be partitioned as $\mathcal{V} = \mathcal{V}_{in} \cup \mathcal{V}_{out} \cup \mathcal{V}_I$, where subsets $\mathcal{V}_{in} = \{1, \dots, N_{in}\}$, $\mathcal{V}_{out} = \{N_{in} + 1, \dots, N_{out}\}$, and $\mathcal{V}_I = \{N_{out} + 1, \dots, N\}$ define the index numbers of inlets, outlets, and interior road elements, respectively. For every road element $i \in \mathcal{V}$, sets

$$\mathcal{I}_i = \{j : (j, i) \in \mathcal{E}\}, \quad (1a)$$

$$\mathcal{O}_i = \{j : (i, j) \in \mathcal{E}\} \quad (1b)$$

define in-neighbors and out-neighbors. Traffic is directed from in-neighbor $j \in \mathcal{I}_i$ towards $i \in \mathcal{V} \setminus \mathcal{V}_{in}$, or it is directed from $i \in \mathcal{V} \setminus \mathcal{V}_{out}$ towards out-neighbor $j \in \mathcal{O}_i$.

III. PROBLEM STATEMENT

We implement the mass-conservation law to obtain traffic dynamics at every road element $i \in \mathcal{V}$. Let $d_i[k]$ denote the external flow, and $\rho_i[k]$, $y_i[k]$, and $z_i[k]$ denote traffic density, network inflow, and network outflow of road $i \in \mathcal{V}$, respectively. Then, traffic dynamics can be defined by

$$\rho_i[k+1] = \rho_i[k] + y_i[k] - z_i[k] + d_i[k] \quad (2)$$

at road element $i \in \mathcal{V}$ where $k = 0, 1, 2, \dots$ denotes the discrete sampling time.

External flow $d_i[k]$ quantifies the traffic inflow entering the NOIR through inlet road element $i \in \mathcal{V}_{in}$, or the traffic outflow leaving the NOIR through outlet road element $i \in \mathcal{V}_{out}$ within time interval $[t_k, t_{k+1}]$. We define $d_i[k]$ as follows:

$$d_i[k] = \begin{cases} u_i[k] \geq 0 & i \in \mathcal{V}_{in} \\ -v_i[k] \leq 0 & i \in \mathcal{V}_{out} \\ 0 & i \in \mathcal{V}_I \end{cases} \quad (3)$$

Network inflow $y_i[k]$ and network outflow $z_i[k]$ are given by

$$y_i[k] = \begin{cases} 0 & i \in \mathcal{V}_{in} \\ v_i[k] & i \in \mathcal{V}_{out}, \\ q_{i,j}[k]z_j[k] & i \in \mathcal{V}_I \end{cases} \quad (4a)$$

$$z_i[k] = \begin{cases} u_i[k] & i \in \mathcal{V}_{in} \\ 0 & i \in \mathcal{V}_{out}, \\ p_i[k]\rho_i[k] & i \in \mathcal{V}_I \end{cases} \quad (4b)$$

where

$$p_i[k] = \begin{cases} 1 & \text{If } i \in \mathcal{V}_{in} \cup \mathcal{V}_{out} \\ 0 & \text{If } i \in \mathcal{V}_I \text{ and } \rho_i = 0 \\ \frac{z_i[k]}{\rho_i[k]} & \text{If } i \in \mathcal{V}_I \text{ and } \rho_i \neq 0 \end{cases} \quad (5)$$

is the outflow probability of road element $i \in \mathcal{V}_I$ at discrete time k , $q_{i,j} \in [0, 1]$ is the fraction of outflow traffic directed from $j \in \mathcal{V} \setminus \mathcal{V}_{out}$ to $i \in \mathcal{O}_j$ at every discrete time k , and

$$\sum_{i \in \mathcal{O}_j} q_{i,j} = 1 \quad (6)$$

at every interior road $i \in \mathcal{V}_I$.

Given the above problem setting, the main purpose of this paper is to alleviate the traffic congestion by assigning the optimal external flow inputs d_1 through $d_{N_{out}}$ minimizing the traffic congestion across the NOIR. Assuming $p_i[k]$ and $q_{i,j}[k]$ are known at every interior road $i \in \mathcal{V}_I$, the external flow is determined by solving a quadratic programming problem with cost function

$$C = \frac{1}{2} \sum_{l=0}^{N_{\tau}-1} \left(\sum_{i \in \mathcal{V}_{in}} u_i^2[k+l] + \sum_{j \in \mathcal{V}_{out}} v_j^2[k+l] \right) \quad (7)$$

and the following inequality and equality constraints:

$$\bigwedge_{l=0}^{N_{\tau}-1} \bigwedge_{i \in \mathcal{V}_{in}} (u_i[k+l] \geq 0), \quad (8a)$$

$$\bigwedge_{l=0}^{N_{\tau}-1} \bigwedge_{j \in \mathcal{V}_{out}} (v_j[k+l] \geq 0), \quad (8b)$$

$$\bigwedge_{l=0}^{N_{\tau}-1} \bigwedge_{i \in \mathcal{V}_I} (\rho_i[k+l] \geq 0), \quad (8c)$$

$$\bigwedge_{l=0}^{N_{\tau}-1} \bigwedge_{i \in \mathcal{V}_I} (\rho_i[k+l] \leq \rho_{i,max}), \quad (8d)$$

$$\bigwedge_{l=0}^{N_{\tau}-1} \left(\sum_{i \in \mathcal{V}_{in}} u_i[k+l] + \sum_{j \in \mathcal{V}_{out}} v_j[k+l] = d_0 \right). \quad (8e)$$

Note that $N_{\tau} < \infty$ is the the time horizon length and $\rho_{i,max}$ is the maximum number of vehicles that can be accommodated at road element $i \in \mathcal{V}_I$. Constraint Eqs. (8a) and (8b) ensure that the traffic back-flow is avoided at every inlet or outlet road element. Constraint (8c) ensures that the solution of the above optimization problem obtains a non-negative traffic

density distribution across the NOIR. Constraint (8d) is imposed to avoid the traffic over-saturation. Assuming the demand for entering and leaving the NOIR is sufficiently high, equality constraint (8e) ensures that d_0 cars can cross the border of the NOIR at every discrete time k .

IV. TRAFFIC NETWORK DYNAMICS

By substituting (3) and (4) in (2), the traffic dynamics at road element $i \in \mathcal{V}$ simplifies to

$$\forall i \in \mathcal{V}_{in} \bigcup \mathcal{V}_{out}, \quad \rho_i[k+1] = \rho_i[k] \quad (9a)$$

$$\forall i \in \mathcal{V}_I, \quad \rho_i[k+1] = (1 - p_i[k]) \rho_i[k] + q_{i,j}[k] p_j[k] \rho_j[k]. \quad (9b)$$

Eq. (9a) shows that the traffic density remains constant at inlet and outlet road elements. Thus, traffic dynamics are not defined over the road element defined by \mathcal{V}_{in} and \mathcal{V}_{out} , and the traffic network dynamics are only defined for the interior road elements.

Assumption 1. Discrete time k represents the time interval $[t_k, t_{k+1})$ where the time increment $\Delta T = t_{k+1} - t_k$ is assumed to be constant for $k = 0, 1, 2, \dots$. We choose a sufficiently-small time increment ΔT such that

$$p_i[k] = \frac{z_i[k]}{\rho_i[k]} \in [0, 1) \quad (10)$$

at every road element $i \in \mathcal{V}_I$ and every discrete time k , if $\rho_i[k] \neq 0$. Note that $p_i[k] = 0$, if $\rho_i[k] = 0$ over the time interval $t \in [t_k, t_{k+1})$ (See Eq. (5)).

To obtain the traffic network dynamics, we define state vector $\mathbf{x} = [\rho_{N_{out}+1} \ \dots \ \rho_N]^T \in \mathbb{R}^{(N-N_{out}) \times 1}$, NOIR inflow vector $\mathbf{y} = [y_{N_{out}+1} \ \dots \ y_N]^T \in \mathbb{R}^{(N-N_{out}) \times 1}$, NOIR outflow vector $\mathbf{z} = [z_{N_{out}+1} \ \dots \ z_N]^T \in \mathbb{R}^{(N-N_{out}) \times 1}$, outflow probability matrix $\mathbf{P} = \text{diag}(p_{N_{out}+1}, \dots, p_N) \in \mathbb{R}^{(N-N_{out}) \times (N-N_{out})}$, and tendency probability matrix $\mathbf{Q} = [Q_{ij}]$ with (i, j) entry

$$Q_{ij}[k] = q_{i+N_{out}, j+N_{out}}[k]. \quad (11)$$

Note that $q_{i+N_{out}, j+N_{out}}[k]$ is the fraction of outflow of road $(j+N_{out}) \in \mathcal{V}_I$ directed towards $(i+N_{out}) \in \mathcal{V}_I$.

Per Eq. (4a), the NOIR inflow vector \mathbf{y} and outflow vector \mathbf{z} can be related to \mathbf{x} by

$$\mathbf{y}[k] = \mathbf{Q}[k] \mathbf{P}[k] \mathbf{x}[k], \quad (12a)$$

$$\mathbf{z}[k] = \mathbf{P} \mathbf{x}[k]. \quad (12b)$$

If Eq. (9b) is applied to model traffic coordination at every interior node $i \in \mathcal{V}_I$, the traffic network dynamics become

$$\mathbf{x}[k+1] = \mathbf{A}[k] \mathbf{x}[k] + \mathbf{B}[k] \mathbf{s}[k], \quad (13)$$

where $\mathbf{s}[k] = [s_i[k]] \in \mathbb{R}^{N_{out} \times 1}$, $\mathbf{B}[k] \in \mathbb{R}^{(N-N_{out}) \times 1}$, $\mathbf{A}[k] \in \mathbb{R}^{(N-N_{out}) \times (N-N_{out})}$ are obtained as follows:

$$s_i[k] = \begin{cases} u_i[k], & \text{If } i \in \mathcal{V}_{in} = \{1, \dots, N_{in}\} \\ v_i[k], & \text{If } i \in \mathcal{V}_{out} = \{N_{in}+1, \dots, N_{out}\} \end{cases}, \quad (14a)$$

$$b_{ij}[k] = \begin{cases} 1 & j \in \mathcal{I}_{i+N_{out}} \\ -1 & j \in \mathcal{O}_{i+N_{out}} \end{cases}, \quad (14b)$$

$$\mathbf{A}[k] = \mathbf{I} - \mathbf{P}[k] + \mathbf{Q}[k] \mathbf{P}[k]. \quad (14c)$$

Theorem 1. Assume graph $\mathcal{G}(\mathcal{V}, \mathcal{E})$ holds the following properties:

- 1) Traffic inflow directs from every inlet boundary road element towards an interior road element.
- 2) There is at least one directed path from every interior node to an outlet node.
- 3) Graph \mathcal{G} contains no isolated node.
- 4) No inlet boundary road element is directly connected to an outlet boundary road element.

Then, the traffic network dynamics (13) is BIBO stable.

Proof: If assumptions of Theorem 1 are satisfied, matrix $\mathbf{A}[k]$ holds the following properties at every discrete time k :

- 1) All entries in matrix $\mathbf{A}[k]$ are non-negative.
- 2) Column i of matrix $\mathbf{A}[k]$ sums up to 1, if $\mathcal{O}_{i+N_{out}} \cap \mathcal{V}_{out} = \emptyset$.
- 3) Elements of column i of matrix $\mathbf{A}[k]$ sums up to a positive number in interval $(0, 1)$, if $\mathcal{O}_{i+N_{out}} \cap \mathcal{V}_{out} \neq \emptyset$.

Thus, eigenvalues of matrix $\mathbf{A}[k]$ are all less than one at every discrete time k . Per traffic dynamics (13), we can define

$$\mathbf{x}[k+1] = \Theta_k \begin{bmatrix} \mathbf{x}[1] \\ \mathbf{B}\mathbf{s}[1] \\ \vdots \\ \mathbf{B}\mathbf{s}[k] \end{bmatrix}, \quad (15)$$

where

$$\Theta_k = [\Gamma_k \ \dots \ \Gamma_1 \ \Gamma_0] \quad (16a)$$

$$\Gamma_h = \prod_{j=k-h+1}^k \mathbf{A}[j] \quad (16b)$$

for $h = 1, \dots, k$, and $\Gamma_0 = \mathbf{I}_{N-N_{out}} \in \mathbb{R}^{(N-N_{out}) \times N-N_{out}}$ is an identity matrix. Because $\mathbf{x}[1] < \infty$, and $\mathbf{s}[k]$ is bounded at every discrete time k , we can write

$$\mathbf{x}[1] \leq z_{\max} \mathbf{1}_{N-N_{out} \times 1}, \quad (17a)$$

$$\mathbf{B}\mathbf{s}[k] \leq z_{\max} \mathbf{1}_{N-N_{out} \times 1}, \quad (17b)$$

where z_{\max} is bounded. If assumptions of Theorem 1 are satisfied, spectral radius of matrix Γ_k is less than $r < 1$ at every discrete time k . Therefore, we can write

$$\begin{aligned} \mathbf{x}^T[k+1] \mathbf{x}[k+1] &\leq z_{\max} \mathbf{1}_{N-N_{out} \times 1}^T \left(\sum_{l=0}^k \sum_{h=0}^k \Gamma_l^T \Gamma_h \right) z_{\max} \mathbf{1}_{N-N_{out} \times 1} \\ &\leq z_{\max}^2 (N-N_{out}) \left(\sum_{l=0}^{\infty} r \right) \leq \frac{z_{\max}^2 (N-N_{out})}{(1-r)}. \end{aligned} \quad (18)$$

This implies that $\mathbf{x}^T[k+1] \mathbf{x}[k+1]$ is bounded at every discrete time k , and thus the BIBO stability of traffic dynamics (13) is proven.

V. TRAFFIC CONGESTION CONTROL

This paper applies the model predictive control (MPC) approach to control congestion through optimizing the boundary inflow and outflow. For the proposed MPC control, we use the linear time-varying dynamics (13) to predict traffic evolution within a future finite time horizon, and determine the optimal boundary external flow as a solution of the quadratic function subject to the inequality and equality constraints.

Given traffic dynamics (13) at discrete time, the following predictive model can be used to model traffic coordination within the next N_τ time steps:

$$\mathbf{X}[k] = \mathbf{G}[k]\mathbf{x}[k] + \mathbf{H}[k]\mathbf{U}[k] \quad (19)$$

where

$$\mathbf{X}[k] = \begin{bmatrix} \mathbf{x}[k+1] \\ \vdots \\ \mathbf{x}[k+N_\tau] \end{bmatrix} \in \mathbb{R}^{(N_\tau N) \times 1} \quad (20a)$$

$$\mathbf{G}[k] = \begin{bmatrix} \mathbf{A}[k] \\ \vdots \\ \mathbf{A}^{N_\tau}[k] \end{bmatrix} \in \mathbb{R}^{(N_\tau N) \times N} \quad (20b)$$

$$\mathbf{H}[k] = \begin{bmatrix} \mathbf{B}[k] & 0 & 0 & \cdots & 0 \\ \mathbf{A}[k]\mathbf{B}[k] & \mathbf{B}[k] & 0 & \cdots & 0 \\ \mathbf{A}^2[k]\mathbf{B}[k] & \mathbf{A}[k]\mathbf{B}[k] & \mathbf{B}[k] & \cdots & 0 \\ \vdots & \vdots & \vdots & \ddots & \vdots \\ \mathbf{A}^{N_\tau-1}[k]\mathbf{B}[k] & \mathbf{A}^{N_\tau-2}[k]\mathbf{B}[k] & \mathbf{A}^{N_\tau-3}[k]\mathbf{B}[k] & \cdots & \mathbf{B}[k] \end{bmatrix} \quad (20c)$$

$$\mathbf{x}[k] = \begin{bmatrix} \rho_1[k] \\ \vdots \\ \rho_N[k] \end{bmatrix} \in \mathbb{R}^{N \times 1} \quad (20d)$$

$$\mathbf{U}[k] = \begin{bmatrix} \mathbf{s}[k] \\ \vdots \\ \mathbf{s}[k+N_\tau-1] \end{bmatrix} \in \mathbb{R}^{(N_\tau N_{out}) \times 1} \quad (20e)$$

Now, we can rewrite the cost function (7) as

$$C = \frac{1}{2} (\mathbf{U}[k]^\top \mathbf{U}[k]). \quad (21)$$

By using the predictive traffic coordination model (19), we can also rewrite the constraint equations (8) as follows:

$$\mathbf{U}[k] \geq \mathbf{0}_{(N_\tau N_{out}) \times 1} \quad (22a)$$

$$\mathbf{G}[k]\mathbf{x}[k] + \mathbf{H}[k]\mathbf{U}[k] \leq \mathbf{1}_{N_\tau \times 1} \otimes \mathbf{x}_{\max} \quad (22b)$$

$$\mathbf{G}[k]\mathbf{x}[k] + \mathbf{H}[k]\mathbf{U}[k] \geq \mathbf{0}_{(N_\tau N) \times 1} \quad (22c)$$

$$(\mathbf{I}_{N_\tau} \otimes \mathbf{1}_{1 \times N_{out}}) \mathbf{U}[k] = d_0 \mathbf{1}_{N_\tau \times 1}, \quad (22d)$$

where $\mathbf{1}_{N_\tau \times 1} \in \mathbb{R}^{N_\tau \times 1}$ and $\mathbf{1}_{1 \times N_{out}} \in \mathbb{R}^{1 \times N_{out}}$ are the one-entry vectors, $\mathbf{0}_{(N_\tau N_{out}) \times 1} \in \mathbb{R}^{(N_\tau N_{out}) \times 1}$ and $\mathbf{0}_{(N_\tau N) \times 1} \in \mathbb{R}^{(N_\tau N) \times 1}$ are the zero-entry vectors, and $\mathbf{I}_{N_\tau} \in \mathbb{R}^{N_\tau \times N_\tau}$ is the identity matrix. Eq. (22a) integrates feasibility conditions (8a) and (8b). Constraint equations (22b), (22c), and (22d) are identical to (8c), (8d), and (8e), respectively.

Theorem 2. If $u_i[k] \geq 0$ at every $i \in \mathcal{V}_{in}$, $v_j[k] \geq 0$ at every $j \in \mathcal{V}_{out}$, $\rho_i[k]$ is updated by dynamics (2), and $\rho_i[0] \geq 0$ at every node $i \in \mathcal{V}_I$, then $\rho_i[k] \geq 0$ at every interior node $i \in \mathcal{V}_I$ and every discrete time k .

Proof: By applying the mass conservation law in (2), traffic network dynamics can be obtained via Eq. (9b) at every interior road $i \in \mathcal{V}_I$. Per Assumption 1, $p_i[k] \in [0, 1]$ at every $i \in \mathcal{V}_I$ and all discrete times k which indicate that $(1 - p_i[k]) > 0$ on the right-hand side of Eq. (9b). Also, $q_{i,j}[k]$ is defined as a quantity in interval $[0, 1]$ at every discrete sampling time k . If $\rho_i[0] \geq 0$, $u_i[k] \geq 0$ at every $i \in \mathcal{V}_{in}$, and $v_j[k] \geq 0$ at every $j \in \mathcal{V}_{out}$, then the right-hand side of Eq. (9b) must be a non-negative quantity at every discrete sampling time k . This implies that $\rho_i[k] \geq 0$ at every node $i \in \mathcal{V}_I$ and discrete time k .

Per Theorem 2, $\rho_i[k] \geq 0$ at every road $i \in \mathcal{V}_I$ and discrete time k . Therefore, condition (22c) is redundant, and conditions (22a), (22b), and (22d) are sufficient to determine the feasible optimal boundary input $\mathbf{U}^*[k]$ by solving the following quadratic programming problem:

$$\min \frac{1}{2} (\mathbf{U}[k]^\top \mathbf{U}[k]) \quad (23)$$

subject to equality constraint (22d) and inequality constraint

$$\begin{bmatrix} -\mathbf{I}_{N_\tau N_{out}} \\ \mathbf{H}[k] \end{bmatrix} \mathbf{U}[k] \leq \begin{bmatrix} \mathbf{0}_{(N_\tau N_{out}) \times 1} \\ \mathbf{1}_{N_\tau \times 1} \otimes \mathbf{x}_{\max} - \mathbf{G}[k]\mathbf{x}[k] \end{bmatrix}. \quad (24)$$

Note that

$$\mathbf{s}^*[k] = [\mathbf{I}_{N_{out}} \ \ \mathbf{0}_{N_{out} \times ((N_\tau-1)N_{out})}] \mathbf{U}^*[k] \quad (25)$$

is the optimal boundary control at discrete time k .

VI. SIMULATION RESULTS

In this section, we present the simulation results of traffic coordination modeling and control in the example NOIR shown in Fig.1. This particular NOIR consists of 259 road elements of Center City Philadelphia where the index numbers of the road elements are shown in Fig. 1. We process the map data generated by SUMO, and obtain the corresponding graph $\mathcal{G}(\mathcal{V}, \mathcal{E})$. Node set $\mathcal{V} = \{1, \dots, 259\}$ can be expressed as $\mathcal{V} = \mathcal{V}_{in} \cup \mathcal{V}_{out} \cup \mathcal{V}_I$ and $\mathcal{V}_{in} = \{1, \dots, 20\}$, $\mathcal{V}_{out} = \{21, \dots, 42\}$, $\mathcal{V}_I = \{43, \dots, 259\}$.

The traffic coordination is simulated for 150 time steps where the outflow probability matrix $\mathbf{P}[k]$ and the fraction probability matrix $\mathbf{Q}[k]$ are randomly generated at every discrete time $k \in \{1, \dots, 150\}$. For simulation, we choose $u_0 = 100$, therefore 100 cars are permitted to cross the boundary of the NOIR shown in Fig. 1 at every discrete time k . For every road $i \in \mathcal{V}_I$,

$$\rho_{i,max} = \frac{n_{i,lane} * l_i}{l_{veh}} \quad (26)$$

assigns an upper bound for the number of cars at road element $i \in \mathcal{V}_I$, where $l_{veh} = 4.5m$ is considered the same for all road elements, l_i is the length of road element $i \in \mathcal{V}_I$ in the Center City area, and $n_{i,lane}$ refers to the number of lanes at road element $i \in \mathcal{V}_I$. Meanwhile, the initial traffic

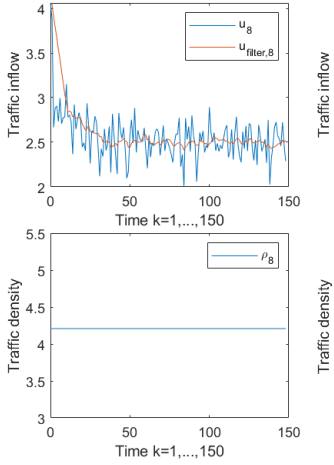


Fig. 2: External traffic inflows and densities of inlet road elements

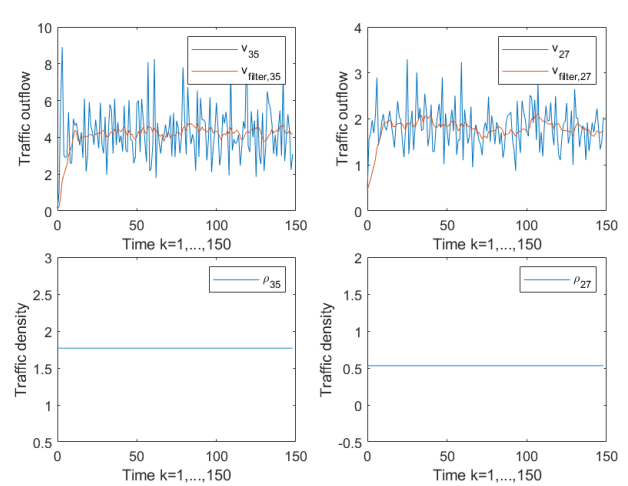
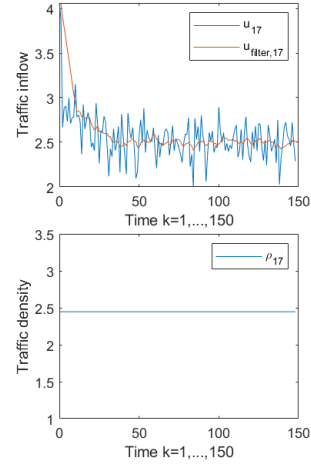


Fig. 3: External traffic outflows and densities of outlet road elements

density $\rho_i[0]$ is assigned randomly for every road element $i \in \mathcal{V}$.

We plot simulation results for two inlet boundary road elements $8 \in \mathcal{V}_{in}$ and $17 \in \mathcal{V}_{in}$, two outlet boundary road elements $27, 35 \in \mathcal{V}_{out}$ and $68 \in \mathcal{V}_I$, and two interior road elements $68 \in \mathcal{V}_I$ and $119 \in \mathcal{V}_I$ in Figs. 2, 3 and 4, respectively. The locations of these six road elements are presented in Table I.

| Road Type | Road Element Index | Name and Location |
|-----------|--------------------|---|
| Inlet | 8 | Cherry St. between N20th St. and N19th St. |
| Inlet | 17 | S11th St. between Locust St. and Walnut St. |
| Outlet | 27 | Cherry St. between N20th St. and N19th St. |
| Outlet | 35 | S11th St. between Locust St. and Walnut St. |
| Interior | 68 | Filbert St. between N12th St. and N13th St. |
| Interior | 119 | John F. Kennedy Blvd. between N16th St. and N17th St. |

TABLE I: Example road elements in NOIR

Fig. 2 and Fig. 3 plot the external traffic flow and traffic density versus discrete time k at inlet road elements $8, 17 \in \mathcal{V}_{in}$ and outlet road elements $27, 35 \in \mathcal{V}_{out}$. It is seen that the traffic density keeps constant at every discrete sampling time k , if road element i is either an inlet ($i \in \mathcal{V}_{in}$) or an outlet ($i \in \mathcal{V}_{out}$). Fig. 4 plots the density variations of the interior road elements $68, 119 \in \mathcal{V}_I$ versus discrete sampling time k . It can be observed that the traffic density reaches the steady-state condition at road elements $68, 119 \in \mathcal{V}_I$ at every discrete time $k > 20$.

Fig. 5 presents the net inflow and outflow of the NOIR versus discrete sampling time k . The red plot illustrates the total number of cars entering the NOIR through all inlets defined by set \mathcal{V}_{in} while the blue plot shows the total number of cars leaving the NOIR through the outlets defined by set

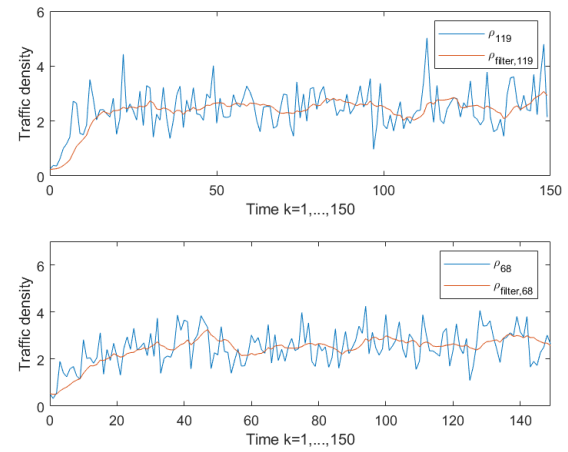


Fig. 4: Traffic density plots for two interior road elements versus discrete time k

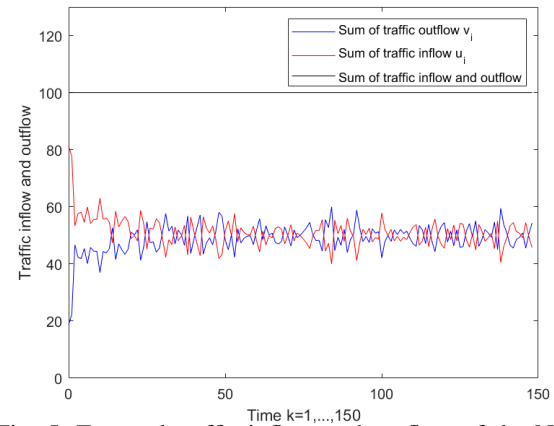


Fig. 5: External traffic inflow and outflow of the NOIR

\mathcal{V}_{out} . The black line indicates that the absolute inflow and outflow sum up to $d_0 = 100$ at every discrete time k . It is also observed that

$$\sum_{i \in \mathcal{V}_{in}} u_i[k] = \sum_{i \in \mathcal{V}_{out}} v_i[k] \cong 50, \quad (27)$$

if $k \geq 30$. This implies that the amount of cars entering the NOIR is approximately equal to the amount of cars departing the NOIR for $k \geq 30$.

VII. CONCLUSION

This paper introduced a conservation-based modeling method to learn the traffic network dynamics and alleviate the traffic congestion. We applied the mass conservation law to model traffic coordination by a time-varying stochastic process where the real map data was used to define the traffic network. We offered an MPC control to manage traffic congestion by controlling the inflow and outflow at the boundary of the NOIR. The simulation results demonstrate that our proposed modeling and control approach can manage the traffic congestion effectively through optimizing the traffic inflow and outflow across the boundary of the NOIR. In our future work, we plan to obtain the traffic dynamics based on real traffic data and control congestion through the boundary ramp meters and traffic signals, situated at road intersections.

VIII. ACKNOWLEDGEMENT

The authors would like to acknowledge the Mechanical Engineering PhD fellowship provided to Xun Liu which was made possible by a generous gift from Dr. Yongping Gu and Fei Gu.

REFERENCES

- [1] C. P. Muneera and K. Karuppanagounder, "Economic impact of traffic congestion- estimation and challenges," *European Transport / Trasporti Europei*, vol. 68.
- [2] M. O'Mahony and H. Finlay, "Impact of traffic congestion on trade and strategies for mitigation," *Transportation Research Board*, vol. 1873, pp. 25–34, 2004.
- [3] L. Ye, Y. Hui, and D. Yang, "Road traffic congestion measurement considering impacts on travelers," *Journal of Modern Transportation*, vol. 21, pp. 28–39, 2013.
- [4] J. Annan, J. Mensah, and N. Boso, "Traffic congestion impact on energy consumption and workforce productivity:empirical evidence from a developing country," *Archives of Business Research*, vol. 3, pp. 40–54, 2015.
- [5] H. Chin and M. Rahman, "An impact evaluation of traffic congestion on ecology," *Planning Studies and Practice*, vol. 3, pp. 32–44, 2011.
- [6] X. Zhang, E. Onieva, A. Perallos, E. Osaba, and V. C. Lee, "Hierarchical fuzzy rule-based system optimized with genetic algorithms for short term traffic congestion prediction," *Transportation Research Part C*, vol. 43, pp. 127–142, 2014.
- [7] T. Ito and R. Kaneyasu, "Predicting traffic congestion using driver behavior," *Procedia Computer Science*, vol. 112, pp. 1288–1297, 2017.
- [8] Z. Huang, J. Xia, F. Li, Z. Li, and Q. Li, "A peak traffic congestion prediction method based on bus driving time," *Entropy*, vol. 21, p. 709, 2019.
- [9] X. Kong, Z. Xu, G. Shen, J. Wang, Q. Yang, and B. Zhang, "Urban traffic congestion estimation and prediction based on floating car trajectory data," *Future Generation Computer Systems*, vol. 61, pp. 97–107, 2016.
- [10] T. Tettamanti, M. T. Horváth, and I. Varga, "Nonlinear traffic modeling for urban road network and related robust state estimation," in *9th European Nonlinear Dynamics Conference (ENOC 2017)*. EUROMECH, 2017, p. 247.
- [11] N. Geroliminis and C. F. Daganzo, "Existence of urban-scale macroscopic fundamental diagrams: Some experimental findings," *Transportation Research Part B: Methodological*, vol. 42, no. 9, pp. 759 – 770, 2008. [Online]. Available: <http://www.sciencedirect.com/science/article/pii/S0191261508000180>
- [12] F. Xu, Z. He, Z. Sha, W. Sun, and L. Zhuang, "Traffic state evaluation based on macroscopic fundamental diagram of urban road network," *Procedia Social and Behavioral Sciences*, vol. 96, pp. 480–489, 2013.
- [13] I. I. Sirmatel and N. Geroliminis, "Integration of perimeter control and route guidance in large-scale urban networks via model predictive control," in *Transportation Research Board 96th Annual Meeting*. Transportation Research Board, 2017, p. 13p.
- [14] Z. Li, S. Jin, C. Xu, and J. Li, "Model-free adaptive predictive control for an urban road traffic network via perimeter control," *IEEE Access*, vol. 7, pp. 172 489–172 495, 11 2019.
- [15] L. Yang, S. Yin, K. Han, J. Haddad, and M. Hu, "Fundamental diagrams of airport surface traffic: Models and applications," *Transportation Research Part B: Methodological*, vol. 106, pp. 29–51, 2017.
- [16] P. Shao, L. Wang, W. Qian, Q.-G. Wang, and X.-H. Yang, "A distributed traffic control strategy based on cell-transmission model," *IEEE Access*, vol. 6, pp. 10 771–10 778, 2018.
- [17] L. Munoz, X. Sun, R. Horowitz, and L. Alvarez-Icaza, "Traffic density estimation with the cell transmission model," vol. 5, 07 2003, pp. 3750 – 3755.
- [18] S. Yin, L. Yang, and K. Han, "Off-block flow optimisation based on cell transmission model," 04 2017.
- [19] O. Feldman and M. Maher, "A cell transmission model applied to the optimisation of traffic signals," 01 2002.
- [20] M. Gregurić, M. Vujić, C. Alexopoulos, and M. Miletić, "Application of deep reinforcement learning in traffic signal control: An overview and impact of open traffic data," *Applied Sciences*, vol. 10, p. 4011, 06 2020.
- [21] Y. Lin, X. Dai, L. Li, and F.-Y. Wang, "An efficient deep reinforcement learning model for urban traffic control," 2018.
- [22] B. Abdulhai, R. Pringle, and G. Karakoulas, "Reinforcement learning for true adaptive traffic signal control," *Journal of Transportation Engineering*, vol. 129, 05 2003.
- [23] P. Mannion, J. Duggan, and E. Howley, *An Experimental Review of Reinforcement Learning Algorithms for Adaptive Traffic Signal Control*, 05 2016, pp. 47–66.
- [24] P. L.A. and S. Bhatnagar, "Reinforcement learning with function approximation for traffic signal control," *Intelligent Transportation Systems, IEEE Transactions on*, vol. 12, pp. 412 – 421, 07 2011.
- [25] H. Rastgoftar and E. Atkins, "An integrative data-driven physics-inspired approach to traffic congestion control," 2019.
- [26] H. Rastgoftar and A. Girard, "Resilient physics-based traffic congestion control," 07 2020, pp. 4120–4125.
- [27] H. Rastgoftar and J.-B. Jeannin, "A physics-based finite-state abstraction for traffic congestion control," 2021.
- [28] S. Lin, B. De Schutter, Y. Xi, and H. Hellendoorn, "Fast model predictive control for urban road networks via milp," *Intelligent Transportation Systems, IEEE Transactions on*, vol. 12, pp. 846 – 856, 10 2011.